Riluzole prevents stress-induced spine plasticity in the hippocampus but mimics it in the amygdala

Saptarnab Naskar [a,c], Siddhartha Datta [a], Sumantra Chattarji [a,b,*]

[a] National Centre for Biological Sciences, Bangalore, 560065, India
[b] Simons Initiative for the Developing Brain and Centre for Discovery Brain Sciences, University of Edinburgh, Edinburgh, EH89XD, UK
[c] Department of Psychiatry and Behavioral Sciences, Northwestern University, Feinberg School of Medicine, 303 E Chicago Ave, Chicago, IL, 60610, USA

ARTICLE INFO

ABSTRACT

Stress elicits divergent patterns of structural plasticity in the amygdala and hippocampus. Despite these contrasting effects, at least one of the immediate consequences of stress – elevated levels of extracellular glutamate – is similar in both brain areas. This raises the possibility that the contrasting effects of stress on neuronal plasticity is shaped by differences in astrocytic glutamate clearance in these two brain areas. Although astrocytes play a key role in glutamate reuptake, past analyses of, and interventions against, stress-induced plasticity have focused largely on neurons. Hence, we tested the impact of riluzole, which potentiates glutamate clearance by astrocytic glutamate transporters, on principal neurons and astrocytes in the basal amygdala (BA) and hippocampal area CA1. Chronic immobilization stress reduced spine-density on CA1 pyramidal neurons of male rats. Riluzole, administered in the drinking water during chronic stress, prevented this decrease; but, the drug by itself had no effect. In contrast, the same chronic stress enhanced spine-density on BA principal neurons, and this effect, unlike area CA1, was not reversed by riluzole. Strikingly, riluzole treatment alone also caused spinogenesis in the BA. Thus, the same riluzole treatment that prevented the effect of stress on spines in the hippocampus, mimicked its effect in the amygdala. Further, chronic stress and riluzole alone decreased the neuropil volume occupied by astrocytes in both the BA and CA1 area. Riluzole treatment in stressed animals, however, did not reverse or further add to this reduction in either region. Thus, while the effects on astrocytes were similar, neuronal changes were distinct between the two areas following stress, riluzole and the two together. Therefore, similar to the impact of repeated stress, pharmacological potentiation of glutamate clearance, with or without stress, also leads to differential effects on dendritic spines in principal neurons of the amygdala and hippocampus. This highlights differences in the astrocytic glutamate reuptake machinery that are likely to have important functional consequences for stress-induced dysfunction, and its reversal, in two brain areas implicated in stress-related psychiatric disorders.

1. Introduction

The debilitating symptoms of stress-related psychiatric disorders are strikingly divergent, characterized by impaired cognitive function alongside enhanced affective symptoms (Chattarji et al., 2015; Geuze et al., 2008; Kitayama et al., 2005; Rauch et al., 2000; Sheline et al., 2001; Woon and Hedges, 2009). Consistent with these clinical observations, animal studies show that exposure to stress elicits contrasting patterns of plasticity across the hippocampus and amygdala (Chattarji et al., 2015; McEwen, 1999; Mitra et al., 2005; Pavlides et al., 2002; Pawlak et al., 2005; Suvrathan et al., 2014; Vyas et al., 2002). For

instance, repeated stress causes loss of dendrites and spines in the hippocampus, but gives rise to dendritic growth and spinogenesis in the basolateral amygdala (Mitra et al., 2005; Pawlak et al., 2005; Vyas et al., 2002). However, the neurobiological underpinnings of these effects remain far from clear. In the search for potential mechanisms underlying these contrasting effects, two broad themes stand out from earlier work. First, at least one of the immediate consequences of stress is similar in both brain areas – glutamate is elevated following exposure to stress (Lowy et al., 1993; Reznikov et al., 2007). Second, despite sharing this common feature in their genesis, the plasticity mechanisms that eventually take shape in neurons and synapses in these two areas exhibit

strikingly different patterns (Chattarji et al., 2015; McEwen et al., 2015). In this context, astrocytes are strategically positioned to respond to the physiological consequences of stress at the level of neurons and their connections. Not only do astrocytes form physical barriers against glutamate spillover from synapses, they also express the glutamate transporter 1 (GLT-1), an important component of the glutamate reuptake machinery (Araque et al., 1999; Khakh and Sofroniew, 2015; Murphy-Royal et al., 2017). This raises the possibility that a key difference between the two areas lies, not only in the neurons, but also in the "first responders" to stress-induced increase in glutamate – the astrocytes. Past analyses, however, have focused largely on neurons.

Could the difference lie in how astrocytes respond to, and process, high levels of glutamate during stress, between the hippocampus and amygdala? As a first step towards addressing this question, we reasoned that pharmacologically-induced enhancement in astrocyte-mediated glutamate clearance should influence the divergent outcomes of stress-induced structural plasticity. Hence, here we explore if and how systemic treatment with riluzole affects the contrasting features of stress-induced plasticity in hippocampal and amygdalar neurons. Among several of its molecular targets that lower extracellular glutamate levels, riluzole potentiates GLT-1 mediated glutamate reuptake (Frizzodos et al., 2004; Fumagalli et al., 2008; Pittenger et al., 2008). Riluzole has been used as a neuroprotective agent for treating amyotrophic lateral sclerosis (ALS) patients (Lacomblez et al., 1996), and has also been reported to have antidepressant effects (Brennan et al., 2010; Pittenger et al., 2008; Sanacora et al., 2007). Moreover, of relevance to the present study, chronic riluzole treatment reversed chronic stress/corticosterone-induced behavioral deficits along with GLT-1 expression, glutamate metabolism and brain derived neurotropic factor (BDNF) in the hippocampus and the prefrontal cortex of rodents (Banasr et al., 2010; Bansal et al., 2021; Gourley et al., 2012). However, little is known about the effects of riluzole, with or without stress, on neuronal and astrocytic morphology in the rodent hippocampus and amygdala. For instance, the same chronic stress leads to opposite effects on spine numbers in neurons of the amygdala and hippocampus. Will chronic systemic administration of riluzole prevent the contrasting effects of stress in both areas? Or alleviate one while exacerbating the other? Will riluzole treatment affect neurons in the two brain areas even in the absence of stress? Further, will the same treatment affect the morphological properties of astrocytes? Would these effects on astrocytes, if any, also vary between the hippocampus and amygdala? Here we address these questions by combining morphometric analyses of spine-density in principal neurons, as well as astrocyte structure, in the basal amygdala (BA) and hippocampal area CA1 using a well-characterized rat model of chronic immobilization stress (Ghosh et al., 2013; Mitra et al., 2005; Rahman et al., 2016; Shukla and Chattarji, 2021; Suvrathan et al., 2014; Vyas et al., 2002).

2. Materials and methods

2.1. Experimental animals

All the experiments were performed on male Sprague Dawley rats. The animals were housed in a 14/10-h light/dark schedule (lights on at 8 a.m.) with *ad libitum* access to food and water. Weaning was done at post-natal day 30. The littermates were housed as 4 animals per home cage. The littermates were segregated into 2 animals per cage around post-natal day 45 and randomly assigned to the different experimental groups. The rats were acclimatized to the experimenter for 10–15 min/cage/day for 3 days prior to the period of experiments. All animal care and experimentation procedures were approved by the CPCSEA (Committee for the Purpose of Control and Supervision of Experiments on Animals), and Institutional Animal Ethics Committee (IAEC) of NCBS, Bangalore.

2.2. Stress protocol

For chronic immobilization stress (CIS), young-adult rats (post-natal day 55–60) were subjected to 2 h of complete immobilization (Mitra et al., 2005) between 10 a.m. and 12 p.m. in plastic immobilization bags for 10 consecutive days. Rats had no access to food or water during this 2-h period. However, they had access to air through a sufficiently large opening at the tip of the immobilization bags adjacent to the rat's nose. After stress, animals were returned to home cages. Age and weight matched control animals were not subjected to any type of stress and were housed in a different room.

2.3. Drug administration

Riluzole (Sigma, St. Louis, MO) was administered to the rats for consecutive 12 days in their drinking water (4 mg/kg body weight/day) (Fig. 1A). The drug administration commenced on the 2nd day of experimenter acclimatization. Riluzole solution (~30 μg/ml, based on average water consumption/cage/day) was prepared by dissolving the drug in drinking water by constant stirring overnight ~6–10 h in a light protected container. Fresh solutions were made every 2 days for the entire duration of the treatment. The daily consumption of water was monitored across all cages throughout the entire duration of the experiment.

2.4. Tissue collection

24 h after completion of the 10 day CIS protocol, the stressed and age-matched control animals (~post-natal day 70) were anesthetized with an overdose of ketamine and xylazine (3:1, 0.9 ml ketamine; 0.3 ml xylazine) and perfused transcardially with 50 ml of 0.1 M phosphate buffer (PB) followed by 100 ml of fixative solution containing 4% 0.1 M sodium phosphate-buffered paraformaldehyde (pH 7.4) (at 4°c). The brains were then gently removed from the skull and post fixation was done for 3 h in the above mentioned fixative (ice cold) on a rocker (at 4°c). Coronal sections of the brain containing the amygdala and dorsal hippocampus were obtained using a vibratome (VT1200, Leica, Germany) and stored in 0.1 M PB for intracellular fills (section thickness: 100 μm).

2.5. Intracellular dye fills of astrocytes and neurons in fixed tissue

The methodology for filling cells in fixed tissue slices was adapted from previously reported protocol (Bushong et al., 2002; Naskar and Chattarji, 2019). The sections, stored PB (at 4°c), were used within 48 h. The sections were placed in cold PB and viewed with an infrared differential interference contrast (DIC)/epifluorescent microscope (SliceScope, Scientifica, UK). The region of interest (Fig. 1B) was identified using a 4× air objective (Olympus, Japan). The cell bodies were identified using a 40× water immersion objective (Olympus, Japan). Sharp glass micropipettes were pulled on a flaming brown pipette puller (P-97/P-1000, Sutter instrument, CA, USA) using thin walled glass capillaries with filament (GC150TF, Harvard apparatus, MA, USA: outer diameter of 1.5 mm and inner diameter of 1.17 mm; resistance ranged between 60 and 100 MΩ) and backfilled with 10 mM Alexa Fluor 488 (for neurons)/568(for astrocytes) hydrazide, sodium salt solution (Thermo Fisher Scientific, CA, USA) (Fig. 1C). The astrocytes and principal neurons were identified by the distinctive size and shape of their soma. The astrocyte soma usually had a round to oval appearance with an approximate diameter of 5 μm whereas the principal neurons had larger cell bodies (diameter: 15 μm) with prominent nucleus and nucleolus visible under DIC. In the dorsal CA1, the astrocytes were dye labelled from the *stratum radiatum,* whereas, the soma of pyramidal neurons were identified and labelled in the *stratum pyramidale.* Unlike the hippocampus. The soma of astrocytes and principal neurons were selected and dye labelled throughout the entire extent of the BA as it is a

non-laminar structure. The somata were impaled, and the dye was injected into the cells by applying a 0.5 s negative current pulse (1 Hz) using Master8 (A.M.P.I. systems, Israel) until the processes were completely filled (~5 min for astrocytes and ~15 min for neurons). The signal from Master8 was fed into a signal isolator unit (Isoflex, A.M.P.I. systems, Israel) and the output was set to ~5 V at constant voltage mode. After several cells were filled in a tissue section, the section was placed in cold 4% paraformaldehyde–PB for 30 min followed by DAPI (Sigma, St. Louis, MO) staining for 15 min. The sections were then mounted in ProlongGold antifade reagent (Thermo Fisher Scientific, CA, USA).

2.6. Image acquisition

Image acquisition was done using high resolution confocal laser scanning microscopy on Olympus Fluoview 3000 (Olympus, Japan) after at least 24 h of mounting. The dye-filled astrocytes were visualized under a 40× oil immersion objective and confocal stacks spanning the entirety of the dye filled cell in all three dimentions were acquired at a Z-step size of 0.5 μm. The Z-step size was in accordance with the Nyquist sampling criteria based on the axial resolution of the imaging setup. The PMT voltage was adjusted for each cell such that the soma was completely saturated. This was done to have a uniform representation of all cells irrespective of minor variations in the amount of dye inside a cell. Primary dendritic segments of dye-filled neurons were visualized under a 60× oil objective and confocal stacks were acquired at a Z-step size of 0.35 μm capturing the dendrite origin point and a dendrite length of ~100 μm.

2.7. Image visualization and analysis

The neuropil volume calculation of dye filled astrocytes was done in FIJI (Schindelin et al., 2012) using a methodology previously described (Naskar and Chattarji, 2019). Briefly, the confocal micrographs were converted to binary format using constant absolute thresholding parameters. The area of non-zero pixels in each optical slice was calculated using the particle analysis plug-in. Using this technique, multiple cross sectional areas consisting of signals only from the astrocytic processes could be calculated spanning the 3D volume occupied by the cell. The neuropil volume was then calculated by multiplying the sum of areas in all optical slices in an image with the Z-step size i.e. 0.5 μm. This method of analysis excludes large, optically resolved spaces occupied by blood vessels, cell bodies and other cellular structures within the territory of the dye filled astrocytes. Arborization profiles of dye filled astrocytes and neuronal spine density were analyzed in Imaris (Oxford instruments, Bitplane, Switzerland) (Fig. 1D-E). The astrocytes were traced and 3D rendered as filaments using the Autopath algorithm. For astrocytes, a seed point threshold of 0.66 μm (size exclusion criteria for local contrast based segmentation algorithm) was used to include all the optically resolved, large astrocytic branches for 3D reconstruction. The volume occupied by astrocytic branches were then subtracted from the total neuropil volume of the respective astrocyte to reveal the volume fraction occupied by the smaller astrocytic leaflets. To quantify spine density, primary dendrites were selected on dye labelled BA principal neurons and pyramidal neurons in the dorsal CA1 region of the hippocampus. The confocal stacks of individual primary dendrites were used to quantify the number of spines using filaments plug-in on Imaris.

2.8. Statistical analysis

All statistical analyses were performed in GraphPad Prism (GraphPad software Inc., La Jolla, CA, USA.). Results are expressed as mean ± SEM (Standard error of the mean). For statistical comparisons, all analyzed dendrites and astrocytes were pooled together from the total number of animals in a given experimental group and the 'n' represents the total number of dendrites and cells respectively. Statistical significance of the effect of CIS and riluzole on dendritic spine density,

astrocyte neuropil volume and volume occupied by astrocytic leaflets were analyzed by 2-way ANOVA followed by post-hoc Tukey's multiple comparison test. Comparisons of segmental distribution of spines in neurons were done by two way repeated measure ANOVA followed by post hoc Sidak's multiple comparisons for each segment.

3. Results

3.1. Chronic riluzole administration prevents stress-induced loss of dendritic spines on hippocampal CA1 pyramidal neurons

We first quantified the impact of chronic immobilization stress (2 h/day for 10 days) on spine numbers on primary apical dendritic branches of dye-labelled CA1 pyramidal neurons of the dorsal hippocampus (Fig. 2A). In agreement with earlier studies (Pawlak et al., 2005), chronic stress led to a significant decrease in the number of spines (Fig. 2B). However, administration of riluzole in the drinking water during chronic stress prevented this reduction in CA1 spine-density in stressed rats (Fig. 2B). Riluzole treatment alone (Control-riluzole) did not result in any change (Fig. 2B: Spines/10 μm: Control: 17.96 ± 0.22; Stress: 15.95 ± 0.25; Control-riluzole: 17.71 ± 0.27; Stress-riluzole: 17.90 ± 0.19, Control: N = 10 animals, 44 dendrites; Stress: N = 10 animals, 43 dendrites; Control-riluzole: N = 10 animals, 44 dendrites; Stress-riluzole: N = 10 animals, 47 dendrites). Further, a detailed analysis of spine-density along 10-μm segments of dendrite revealed how the stress-induced spine loss, and its prevention by riluzole, is distributed across primary apical dendrites. Dendritic segments extending between 20 and 80 μm from the origin of the branch had significantly lower spine numbers as a result of chronic stress (Fig. 2C). However, riluzole alone, and when administered during stress, resulted in spine numbers comparable to control levels (Fig. 2C).

3.2. Riluzole treatment alone causes spinogenesis, but does not prevent stress-induced spine formation, on BA principal neurons

In contrast to spine loss in area CA1, the same chronic stress resulted in a significant increase in spine numbers on BA principal neurons (Fig. 2D–F), as has been reported in earlier (Mitra et al., 2005; Padival et al., 2013). Notably, riluzole administration alone also resulted in a significant increase in spine-density on BA principal neurons (Fig. 2E, Control-riluzole), similar to stress-induced spinogenesis in the BA but unlike what we find in area CA1. BA spine-density in animals that received riluzole treatment during chronic stress (Stress-riluzole) remained at levels that are significantly higher than BA neurons in unstressed control animals, but comparable to levels seen after exposure to chronic stress alone (Fig. 2E). Also, the two interventions together – riluzole administration in stressed animals – prevented further stress-induced increase in BA dendritic spine numbers (Fig. 2E: Spines/10 μm: Control: 12.77 ± 0.26; Stress: 13.93 ± 0.22; Control-riluzole: 15.66 ± 0.21; Stress-riluzole: 14.49 ± 0.31, Control: N = 8 animals; 50 dendrites, Stress: N = 8 animals; 54 dendrites, Control-riluzole: N = 8 animals; 55 dendrites, Stress-riluzole: N = 7 animals; 32 dendrites). Analysis of spine-density in steps of 10-μm segments along the dendrite revealed changes in the distribution of spines across all four experimental groups (Fig. 2F).

3.3. Changes in astrocytic morphology are similar in the BA and CA1 area following stress, riluzole and the two together

We next asked the following questions. First, does riluzole affect astrocyte morphology in the hippocampus and the amygdala? Second, does chronic stress affect astrocyte morphology and if so, does riluzole have any impact on these stress-induced changes? To this end, we examined the effect of the same chronic riluzole administration on astrocytes in the CA1 area and BA from the same brain tissue used earlier for the spine analyses. Specifically, we quantified the neuropil volume
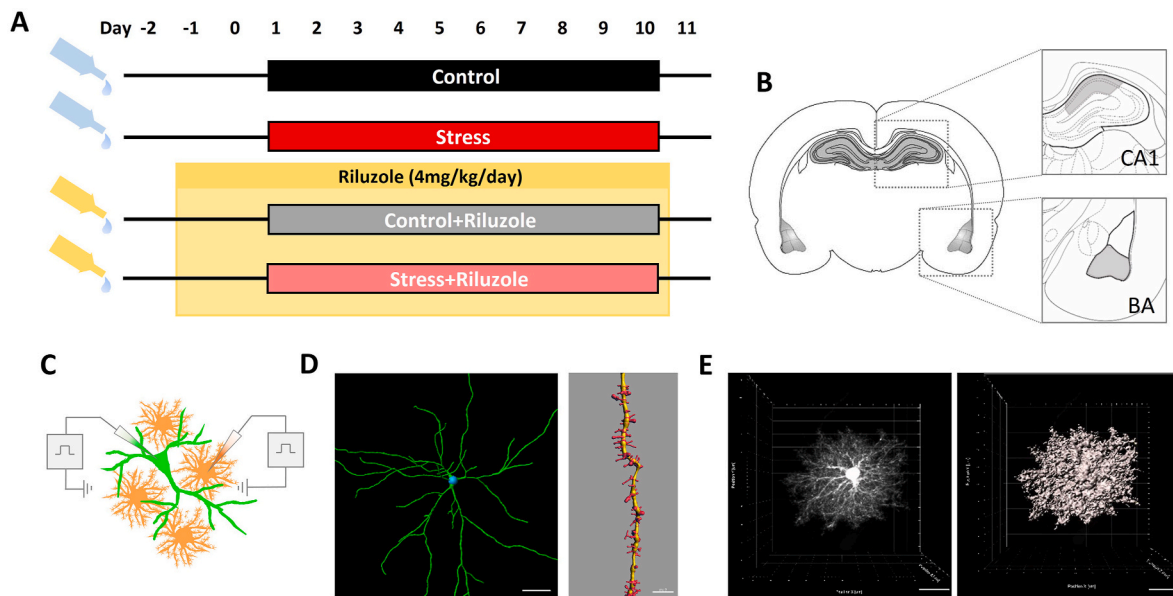
Fig. 1. Experiment design and analysis (A) Animals were randomly assigned to four experimental groups. The *Control* and *Stress* groups received regular drinking water throughout whereas the *Control-Riluzole* and *Stress-Riluzole* groups received riluzole in their drinking water for consecutive 12 days (4 mg/kg/day). Both the *Stress* and *Stress-riluzole* groups were subjected to 2 h of immobilization for 10 consecutive days. (B) A rat brain coronal section depicting brain regions within which quantitative cellular morphometry was performed. (C) Individual neurons and astrocytes were iontophoretically dye labelled with alexa-fluor 488 and 568 solution respectively. (D) 3D reconstructions of dye labelled principal neurons (left) and their primary dendrite segment (right). (E) A representative confocal micrograph of a dye-labelled astrocyte (left) and its 3D territorial reconstruction (right).

occupied by the astrocytes, as well as the volume fractions occupied by the small astrocytic leaflets that form the tri-partite synapse (Khakh and Sofroniew, 2015). In striking contrast to the changes seen in neurons, both chronic stress and riluzole administration had similar effects on CA1 astrocytes (Fig. 3A). Stress and riluzole, each on their own, resulted in a significant reduction in the neuropil volume occupied by astrocytes (Fig. 3B, Volume (μm^3), Control: 72316 ± 1853 μm^3, Stress: 62606 ± 1611 μm^3, Control-riluzole: 60667 ± 1727 μm^3, Stress-riluzole: 62795 ± 1544 μm^3, Control: N = 10 animals, 52 cells, Stress: N = 10 animals, 47 cells, Control-riluzole: N = 10 animals, 53 cells, Stress-riluzole: N = 10 animals, 50 cells). Moreover, riluzole administration to animals undergoing chronic stress (Stress-riluzole) occluded any further reduction in CA1 astrocyte volume compared to the Control-riluzole group evidenced by a significant interaction observed in the two-way ANOVA. (Fig. 3B: Interaction: p = 0.0006).

Similar to the effects in area CA1, riluzole treatment by itself (Control-riluzole) also resulted in a significant decrease in the overall neuropil volume occupied by BA astrocytes compared to vehicle-treated controls. And exposure to chronic stress led to similar reductions in BA astrocytic neuropil volume (Fig. 3E: Volume (μm³), Control: 48925 ± 2663 μm3, Stress: 39459 ± 2518 μm³, Control-riluzole: 36484 ± 1600 μm³, Stress-riluzole: 36589 ± 1607 μm³, Control: N = 8 animals, 31 cells, Stress: N = 8 animals, 34 cells, Control-riluzole: N = 8 animals, 27 cells, Stress-riluzole: N = 7 animals, 31 cells.). Notably, in both brain areas, chronic riluzole administration to animals undergoing chronic stress (Stress-riluzole) did not reverse the reduced astrocyte neuropil volume back to control levels. Also, there was no significant difference in the mean values for neuropil volumes between Stress-riluzole and Stress groups, suggesting an occlusion effect as evidenced by a significant interaction observed in the two-way ANOVA (Fig: 3 E: Interaction: p = 0.0331).

Finally, we assessed the volume fractions occupied by the small astrocytic leaflets. Stress led to a significant reduction in the volume occupied by the astrocytic leaflets in the CA1 area and BA (Fig. 3). Although riluzole administration alone mimicked the effects of chronic stress on these two measures, when these two treatments were combined (i.e. Stress-riluzole), no further changes were seen in the volume of

astrocytic leaflets (Fig. 3C and F). Further, the effect of stress and riluzole administration on astrocytic leaflets was more pronounced in the CA1 area than the BA (Fig. 3C & F: Volume occupied by astrocytic leaflets (μm³), CA1: Control: 60782 ± 1626 μm³, Stress: 52911 ± 1404 μm³, Control-riluzole: 50648 ± 1493 μm³, Stress-riluzole: 52214 ± 1337 μm³; BA: Control: 41054 ± 2087 μm³, Stress: 32573 ± 1616 μm³, Control-riluzole: 31291 ± 1455 μm³, Stress-riluzole: 32091 ± 1359 μm³).

4. Discussion

Decades of analyses using a range of rodent models of stress have given rise to a powerful framework for understanding the mechanisms, and consequences, of stress-induced plasticity across biological scales (Chattarji et al., 2015; Roozendaal et al., 2009). Most of these foundational studies were centered on neurons, with an initial focus on the hippocampus (McEwen, 1999). Here we present findings that add a new dimension to this framework in two ways. First, we explored a potential role for astrocytic reuptake of glutamate in stress-induced modulation of spine numbers, which remains largely unexplored despite growing evidence for a role for astrocytes in both health and disease (Allaman et al., 2011; MacVicar and Newman, 2015; Murphy-Royal et al., 2017, 2019; Sofroniew and Vinters, 2010). Second, motivated by previously reported differences in the impact of stress on the amygdala versus hippocampus (Chattarji et al., 2015), we also examined how the outcomes of stress, and pharmacological modulation of extracellular glutamate, varies across neurons and astrocytes between these two brain areas. Consistent with earlier reports, changes in neurons after chronic stress were opposite, as evidenced by a decrease in spine numbers in the CA1 area (Fig. 4A), but an increase in the BA (Fig. 4B). On the other hand, the effects of stress on astrocytes were similar – a reduction in neuropil volume occupied by individual astrocytes in both the BA and area CA1; a similar decrease was also seen following chronic riluzole administration (Fig. 4A and B). In neurons, however, riluzole elicited strikingly divergent effects. Although chronic riluzole treatment had no effect on CA1 spine-density, it actually led to spinogenesis in the BA, similar to what stress elicits by itself. Finally, the combined impact of the two
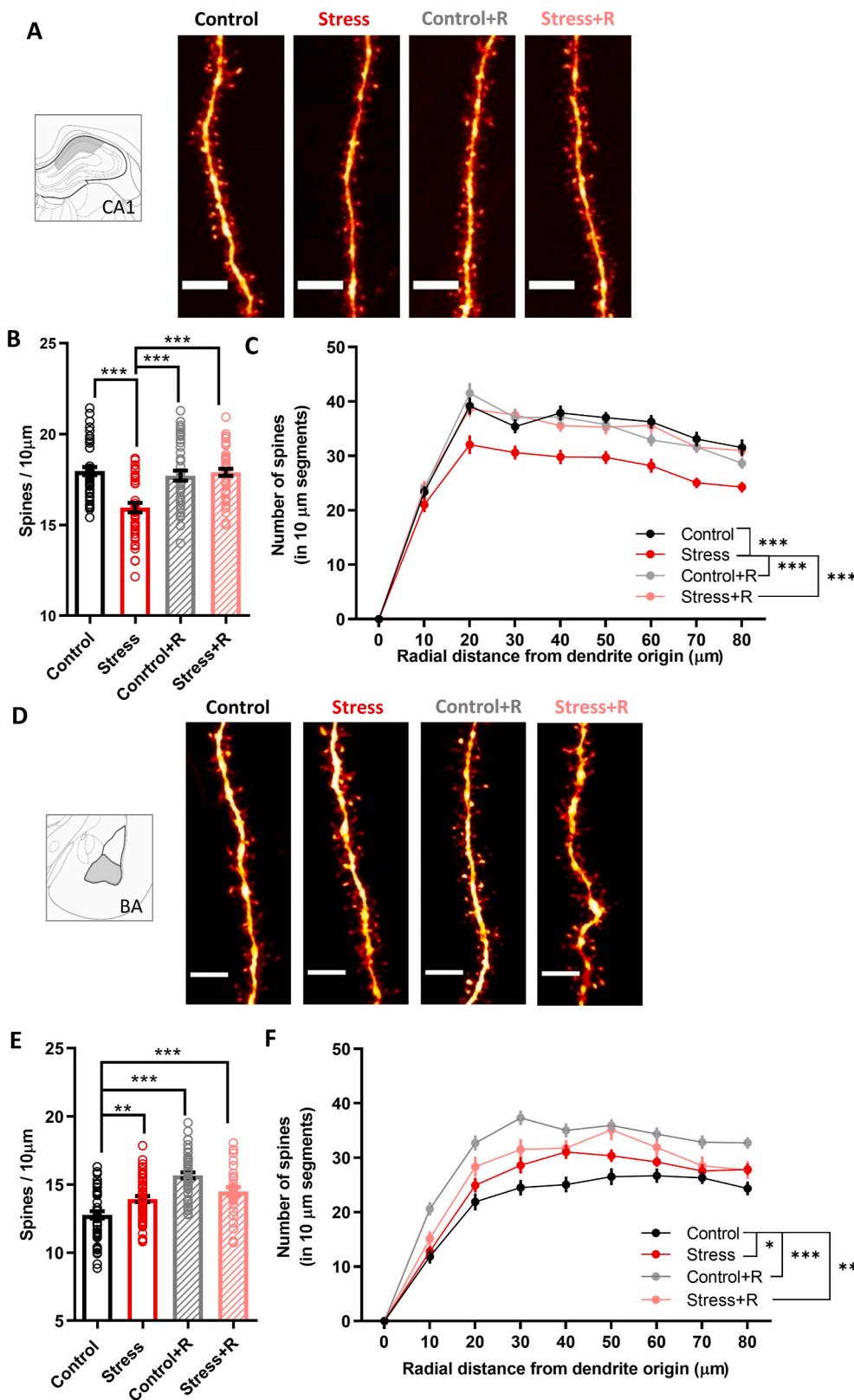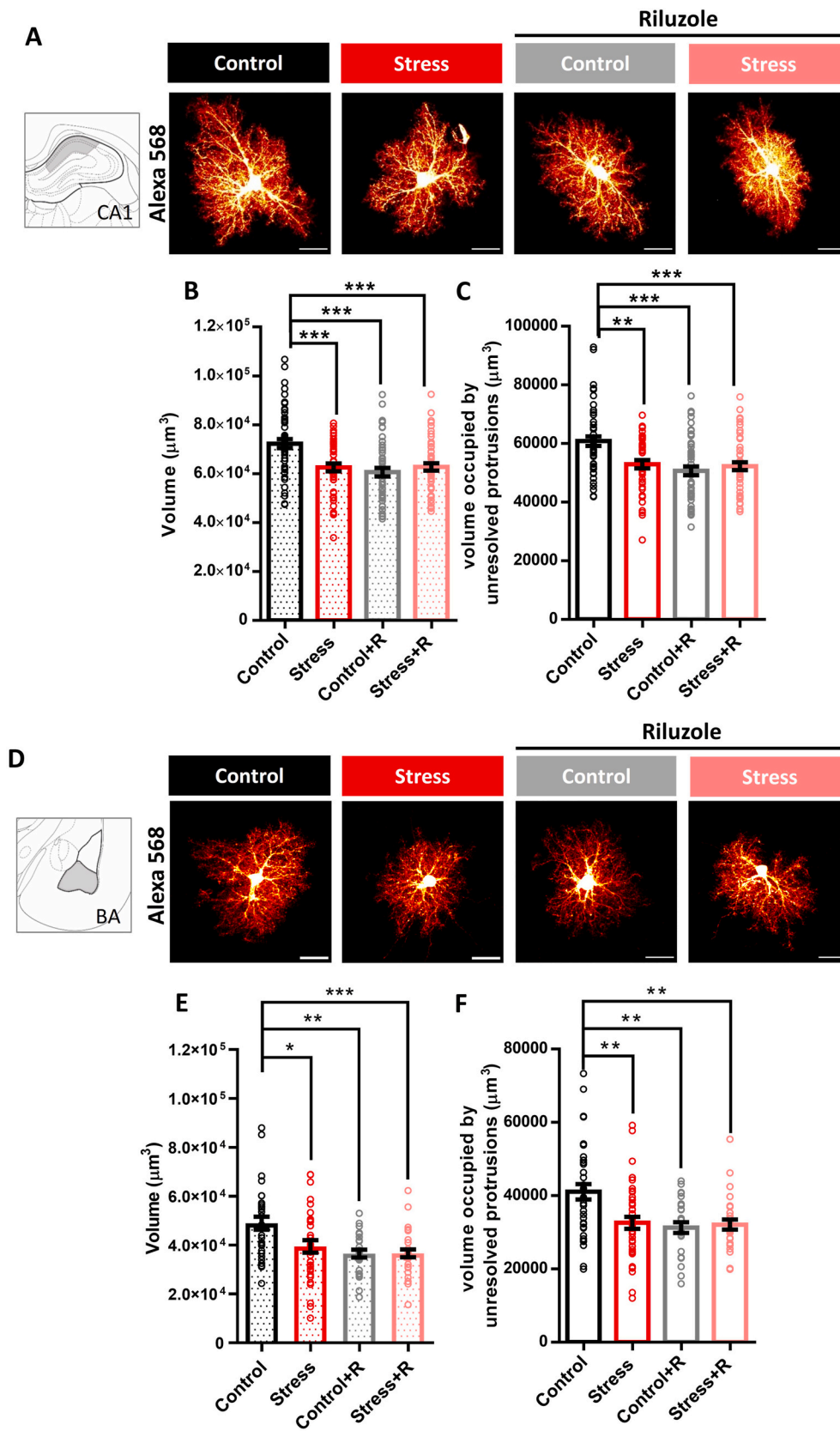
Fig. 2. Effects of chronic riluzole administration and stress on CA1 and BA neuronal spine density and distribution (A) Representative confocal images of CA1 pyramidal neuron primary apical dendrite segments and spines across different experimental groups. (B) Mean (±SEM) values of spine density (calculated as average number of spines per 10 μm dendritic segment) in the primary dendrites of CA1 pyramidal neurons of the four experimental groups (Two-way ANOVA, Stress: F (1,174) = 14.68, p = 0.0002; Riluzole: F (1,174) = 12.56, p = 0.0005; Interaction: F (1,174) = 21.2, p < 0.0001, post-hoc Tukey's multiple comparisons test: Control vs. Control-riluzole: p = 0.8779; Control vs. Stress-riluzole: p = 0.9969; Control vs. Stress: p < 0.0001; Control-riluzole vs. Stress: p < 0.0001; Control-riluzole vs. Stress-riluzole: p = 0.9456, Stress vs. Stress-riluzole: p = 0.0001, ***p < 0.001) (C) Segmental analysis of the mean (±SEM) number of spines in successive 10 μm segments along the primary dendrite of the CA1 pyramidal neurons as a function of increasing distance from the dendrite origin in the four experimental groups (Two-way RM ANOVA, Control vs. Stress: F (1, 85) = 31.84, p < 0.0001; Stress vs. Control-riluzole: F (1, 85) = 22.64, p < 0.0001, Stress vs. Stress-riluzole: F (1, 88) = 32.81 p < 0.0001, Control vs. Control-riluzole: F (1, 86) = 0.2485, p = 0.6194; Control vs. Stress-riluzole: F (1, 89) = 0.2426, p = 0.6236; segments were compared using post-hoc Sidak's multiple comparisons test, ***p < 0.001). (D) Representative confocal images of BA principal neuron primary dendrite segments and spines across different experimental groups. (E) Mean (±SEM) values of spine density (calculated as average number of spines per 10 μm dendritic segment) in the primary dendrites of BA principal neurons of the four experimental groups (Two-way ANOVA, Stress: F (1,187) = 0.0008, p = 0.9771; Riluzole: F (1,187) = 46.27, p < 0.0001; Interaction: F (1,187) = 21.2, p < 0.0001, post-hoc Tukey's multiple comparisons test: Control vs. Control-riluzole: p < 0.0001; Control vs. Stress: p = 0.0037; Control vs. Stress-riluzole: p < 0.0001,**p < 0.01, ***p < 0.0001) (F) Segmental analysis of the mean (±SEM) number of spines in successive 10 μm segments along the primary dendrite of the BA principal neurons as a function of increasing distance from the dendrite origin in the four experimental groups (Two-way RM ANOVA, Control vs. Stress: F (1, 94) = 6.284, p = 0.0139; Control vs. Control-riluzole: F (1, 96) = 60.44, p < 0.0001; Control vs. Stress-riluzole: F (1, 73) = 12.50, p = 0.0007; post-hoc Sidak's multiple comparisons test, *p < 0.05, **p < 0.01, ***p < 0.001). Scale bar: 5 μm.

interventions was also distinct – stress-induced CA1 spine loss was reversed to control levels by riluzole (Fig. 4A), but stress-induced increase in BA spine numbers remained significantly higher than control levels even after riluzole treatment (Fig. 4B). Thus, pharmacological attenuation of extracellular glutamate, both in the presence and absence

of repeated stress, gives rise to differential effects on dendritic spines in CA1 and BA neurons; but the effects on astrocyte morphology are similar across the two areas.

The brain region-specific differences in spine plasticity, following stress and riluzole alone, are interesting for several reasons. First, it

Fig. 3. Effects of chronic riluzole administration and stress on the volume and morphology of the CA1 and the BA astrocytes. (A) Representative confocal images of individual astrocytes labelled with Alexa fluor 568 in the CA1 region of the dorsal hippocampus. (B) Mean (±SEM) values of the overall territorial volume occupied by CA1 astrocytes across four experimental groups (Two way ANOVA, Stress: $F_{(1, 198)} = 4.979$, $p = 0.0268$, Riluzole: $F_{(1, 198)} = 11.38$, $p = 0.0009$; Interaction: $F_{(1, 198)} = 12.14$, $p = 0.0006$; post-hoc Tukey's multiple comparison test: Control vs Stress: $p = 0.0005$, Control vs. Control-riluzole: $p < 0.0001$, Control vs. Stress-riluzole: $p = 0.0006$, Control-riluzole vs Stress-riluzole: $p = 0.9385$, ***$p < 0.001$). (C) Mean (±SEM) values of the volume occupied by the fine astrocytic leaflets across four experimental groups in CA1 (Two way ANOVA, Stress: $p = 0.0342$, Riluzole: $p = 0.0003$, Interaction: 0.0016; post-hoc Tukey's multiple comparison test: Control vs Stress: $p = 0.0014$, Control vs. Control-riluzole: $p < 0.0001$, Control vs. Stress-riluzole: $p = 0.0003$, Control-riluzole vs Stress-riluzole: $p = 0.8737$, **$p < 0.01$, ***$p < 0.001$). (D) Representative confocal images of individual astrocytes labelled with Alexa fluor 568 in the basal amygdala (BA). (E) Mean (±SEM) values of the overall territorial volume occupied by BA astrocytes across four experimental groups (Two-way ANOVA, Stress: $F_{(1, 119)} = 4.446$, $p = 0.0371$, Riluzole: $F_{(1, 119)} = 11.89$, $p = 0.0008$, Interaction: $F_{(1, 119)} = 4.647$, $p = 0.0331$; post-hoc Tukey's multiple comparisons test: Control vs Stress: $p = 0.0125$, Control vs. Control-riluzole: $p = 0.0011$, Control vs. Stress-riluzole: $p = 0.0007$, *$p < 0.05$, **$p < 0.01$, ***$p < 0.001$). (F) Mean (±SEM) values of the volume occupied by the fine astrocytic leaflets across four experimental groups in BA (Two way ANOVA, Stress: $p = 0.0310$, Riluzole: $p = 0.0043$, Interaction: 0.0094; post-hoc Tukey's multiple comparison test: Control vs Stress: $p = 0.0016$, Control vs. Control-riluzole: $p = 0.0011$, Control vs. Stress-riluzole: $p = 0.0026$, Control-riluzole vs Stress-riluzole: $p = 0.9909$, **$p < 0.01$). Scale bar: 20 μm.
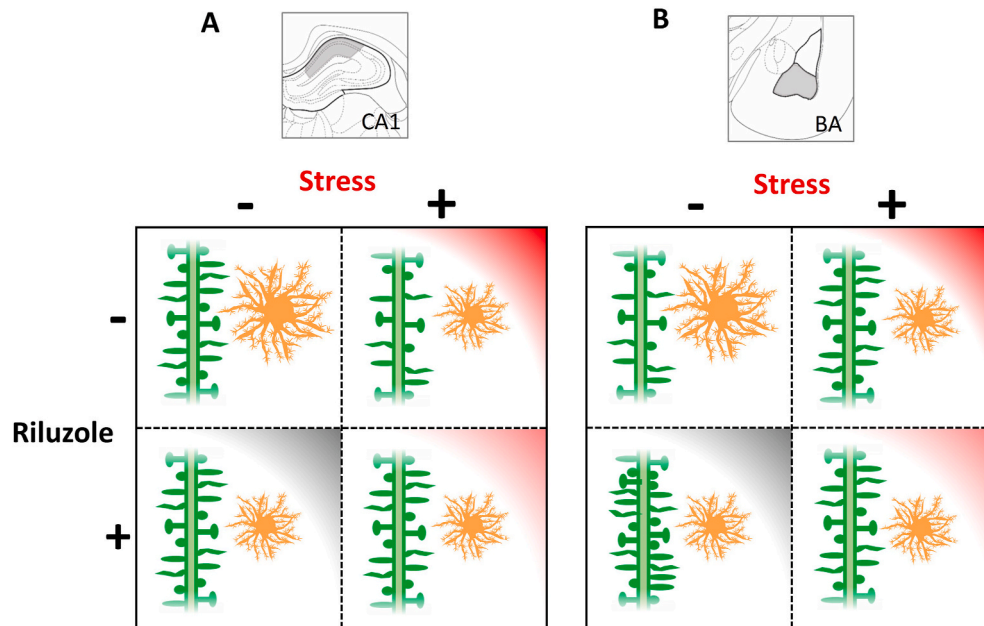
Fig. 4. Summary of experimental findings. (A) Effects of chronic riluzole and/or Stress on spine density and astrocytic morphology in the dorsal CA1 region of the hippocampus. (B) Effects of chronic riluzole and/or Stress on spine density and astrocytes morphology in the basal amygdala.

raises the possibility that baseline levels of glutamate and its modulation, even in the absence of stress, may differ between the hippocampus and amygdala because the same systemic pharmacological reduction in extracellular glutamate leads to different effects on spine numbers in the two areas. Second, the differential effects of the same pharmacological manipulation of glutamate also extends to stress. Finally, the divergent impact is evident in neurons, not astrocytes. It is however, important to underline here that riluzole acts on several targets which has the net effect of reducing extracellular levels of glutamate (Pittenger et al., 2008). Apart from potentiating glutamate uptake via GLT-1, riluzole can, for instance, also act as an NMDAR and AMPAR antagonist that dampens the post-synaptic response to extracellular glutamate (Debono et al., 1993; Zona et al., 2002). However, these targets are relatively low affinity requiring higher concentrations of riluzole to be effective. By contrast, the astrocytic glutamate transporter is a high affinity target of riluzole such that relatively lower concentrations of can effectively potentiate glutamate transport via GLT-1 (Frizzodos et al., 2004). In our study, the concentration of riluzole used is comparable to the EC50 of riluzole's action on GLT-1. Therefore, the effects of riluzole on cellular morphology reported here is most likely due to its action on astrocytic glutamate transport. That being said, further investigations are necessary to ascertain if targeted modulation of astrocytic glutamate transport alone is sufficient to occlude/reverse the effects of stress. Astrocytic GLT-1 is involved in approximately 90% of the glutamate reuptake from the synaptic and extra-synaptic space (Rothstein et al., 1996; Tanaka et al., 1997). Interestingly, regionally selective knock-down of GLT-1 in the infralimbic cortex alone is sufficient to induce depression-like behavior in rodents (Fullana et al., 2019). Hence, region-specific differences in stress-induced alteration in territorial coverage of astrocytes (Naskar and Chattarji, 2019) is likely to affect astrocytic glutamate re-uptake, extracellular glutamate availability, and extra-synaptic spill-over. Apart from differential territorial coverage by astrocytes, other studies have highlighted region-specific variations in the effects of chronic stress on GLT-1 mRNA expression. For example, chronic restraint stress increased GLT-1 mRNA and protein expression in the hippocampus (Reagan et al., 2004), but chronic unpredictable stress did not affect GLT-1 mRNA levels in the prefrontal cortex (Banasr et al., 2010). This may also have functional implications for other measures of stress-induced synaptic plasticity. For example, repeated stress, which

causes spine loss, also impairs hippocampal long-term potentiation (LTP) (Foy et al., 1987; Pavlides et al., 2002). By contrast, chronic stress enhances LTP in the basolateral amygdala (Suvrathan et al., 2014). Moreover, inhibition of the NMDA receptor, which mediates LTP, also prevents the opposite forms of stress-induced structural plasticity in both brain areas (Magariños and McEwen, 1995; Yasmin et al., 2016).

The relationship between synaptic/extra synaptic glutamate concentrations, glutamate uptake and morphology of neurons/astrocytes is an actively investigated field of research. An important consideration comes from a series of studies that highlight heterogeneity in the percentage of synapses that are enwrapped by astrocytic processes (ranging from about 30 to 90% depending on the brain area) (Zhou et al., 2019). To that end, synaptic activity or the physical size of a post-synaptic compartment is inversely related to the astrocytic coverage (Henneberger et al., 2020; Herde et al., 2020). However, results from theoretical simulations suggested that glutamate clearance from synapses through high-affinity glutamate transporters is unaffected by changes in the tissue geometry (Savtchenko et al., 2021). Additionally, several reports underline the concomitance of altered GLT-1 expression and neurodegeneration associated with ALS and epileptic seizures (Hubbard et al., 2016; Proper et al., 2002; Rothstein et al., 1995). Astrocytes play crucial role in both synaptogenesis as well as synaptic pruning through several soluble and contact signaling molecules (Allen and Eroglu, 2017; Boisvert et al., 2018). Therefore, the impact of altered glutamate clearance on the cyto-architecture of astrocytes and neurons can be mediated through a combination of indirect mechanisms. Our findings underscore the need for more detailed analyses of how stress affects interactions between these multiple factors.

Apart from its effects on glutamate levels in and around the synapse, the use of riluzole is also relevant from a therapeutic perspective. A growing body of research, in both humans and pre-clinical rodent models, points to the potential use of riluzole as an antidepressant (Banasr et al., 2010; Bansal et al., 2021; Brennan et al., 2010; Gourley et al., 2012; Pittenger et al., 2008; Sanacora et al., 2007; Spangler et al., 2020). As depression-like symptoms are often precipitated by some form of stress, animal models of stress have been used extensively to investigate cellular mechanisms of depression. It is especially interesting to note that while amygdalar spinogenesis is triggered by both stress and riluzole separately, it is occluded when administered together. In the

hippocampus, by contrast, riluzole prevents the effects of stress on hippocampal spines. This has interesting parallels with a study in which amygdalar spinogenesis, triggered by chronic stress, were also occluded by transgenic overexpression of the neurotrophin BDNF (Govindarajan et al., 2006). Strikingly, BDNF overexpression also caused antidepressant effects and prevented chronic stress-induced hippocampal atrophy in the same mice (Govindarajan et al., 2006). Riluzole also leads to up-regulation of BDNF expression in the hippocampus (Katoh-Semba et al., 2002; Pereira et al., 2017). It remains to be explored whether or not, riluzole has similar effects on BDNF in the amygdala. In another study, tianeptine, an antidepressant with proven clinical efficacy, reduced NMDAR currents, without affecting AMPAR currents, in amygdala neurons. By contrast, tianeptine enhanced both NMDAR and AMPAR currents in area CA1 (Pillai et al., 2012). Thus, the same antidepressant treatment elicited contrasting patterns of changes in excitatory glutamatergic synaptic currents in the amygdala versus hippocampus. Therefore, analysis of the mechanisms behind differential effects of these antidepressant interventions on hippocampal and amygdalar plasticity would provide further insights into novel therapeutic targets for alleviating symptoms of stress-related psychiatric disorders.

Stress leads to consistent systemic responses (elevation of systemic corticosterone) spanning across a wide range of age groups in rats (<1 month to 27 months) (Gilles et al., 1996; Sapolsky et al., 1983). However, post stress recovery is significantly impaired in older rats (Sapolsky et al., 1983). In addition to that, aging can alter astrocytic morphology and transcriptomic signatures that can impact several aspects of synaptic plasticity (Boisvert et al., 2018; Grosche et al., 2013). Therefore, age of the subjects can greatly influence the outcomes of stress. Although our study illuminates an important aspect of the relationship between glutamate reuptake, stress and morphological plasticity, it is limited by the fact that only male rats were used here. Baseline circulating levels of glutamate and glutamate transport via astrocytic transporters can be differentially modulated by sex differences and stages of the estrous cycle (Giacometti and Barker, 2020). Sex differences in the circulating gonadal hormones, and other transcriptomic variables, can also influence susceptibility to, and outcomes of, stress exposure (Gould et al., 1990; Seney et al., 2022; Wellman et al., 2018). For instance, the impact of stress on hippocampal dendritic spines and hippocampus-dependent cognitive tasks differ between male and female rats (Luine et al., 2017; Shors et al., 2001). Moreover, both single and repeated stress paradigms elicit gender-dependent variations in fear expression and synaptic plasticity in the basolateral amygdala (Blume et al., 2019; Gupta and Chattarji, 2021). Therefore, further investigations will be needed to address the sex dependent heterogeneity in astrocyte mediated glutamate uptake and its influence on stress-induced neuronal plasticity.

In conclusion, earlier analyses of aberrations caused by stress, and strategies to reverse them, were aimed primarily at understanding synaptic and molecular signaling abnormalities in neurons. Here we report a potential role for astrocytic reuptake of extracellular glutamate in both correcting and mimicking stress-induced spine plasticity in CA1 and BA neurons respectively, thereby shifting the focus to astrocytes in what was traditionally thought of as neuronal dysfunction. Together, these findings open up possibilities of identifying potential therapeutic targets against stress-induced alterations in neuron-astrocyte interactions.

Preamble

The study described here, like other papers from my laboratory, is a testament to the deep impact Bruce McEwen's intellect and generous spirit had on the way I and my younger colleagues thought about, and did, science in Bangalore, India. Our interactions began when Bruce invited me to his lab at Rockefeller University sometime around 2001. At that first meeting I described to him our discovery of how the same chronic stress that caused CA3 dendritic atrophy in the hippocampus, elicited dendritic growth the basolateral amygdala. That visit paved the way for almost two decades of stimulating interactions and fruitful collaborations that involved many students and post-docs from my lab, who all benefited immensely from his mentorship and encouragement. This article describes work that, in some ways, comes full circle since that first meeting in Bruce's lab. It revolves around a question that Bruce and I grappled with for years – what is fundamentally different between hippocampal and amygdalar neurons that leads to the contrasting effects of stress? Over the course of several discussions with Bruce around 2014–15, I suggested to him that it is curious how stress caused loss of dendrites and spines in laminar structures (i.e. hippocampus and prefrontal cortex), but the opposite effect in the amygdala, a non-laminar, nuclear structure. He noted that despite these contrasting effects, the initial impact of stress is similar in all three areas – elevated levels of glutamate. I then went on to ask him – since astrocytes play a critical role in mopping up the excess glutamate – what if the astrocytes themselves are somehow "different" in laminar versus non-laminar structures? Needless to say, as a Physics dropout I knew next to nothing about astrocytes or glutamate transporters. But, the beauty of learning from Bruce lay in the fact that I could float any crazy idea and he'd show me ways to think about it and give it concrete shape – all through his astonishing depth and breadth of knowledge – and his patience and encouragement to pursue an idea. Soon after, in characteristic fashion, Bruce introduced me to experts who could address some of the questions about astrocyte structure and function. And of course, my inbox filled up with emails from Bruce, with all the papers I needed to read up on. But, his mentorship and guidance was not just limited to "big picture" advice – he also helped us design experiments and provided us with all the necessary technical details. This is how, over the course of months and years – through countless emails and many phone calls a week – our work continued across New York and Bangalore. And as the data emerged, Bruce went over every detail, and gave us valuable advice. Because of how deeply engaged he was with our work, it never felt like we were halfway around the world. He was there for us, always. This article is yet another example of how Bruce nurtured our work with his wisdom, patience and kindness.

CRediT authorship contribution statement

Saptarnab Naskar: Conceptualization, Methodology, Validation, Formal analysis, Investigation, Data curation, Writing – original draft, Writing – review & editing, Visualization. **Siddhartha Datta:** Formal analysis, Investigation, Data curation, Visualization. **Sumantra Chattarji:** Conceptualization, Resources, Writing – original draft, Writing – review & editing, Supervision, Project administration, Funding acquisition.

Declaration of competing interest

The authors declare no competing financial interest.

Data availability

Data will be made available on request.

Acknowledgments

References

Allaman, I., Bélanger, M., Magistretti, P.J., 2011. Astrocyte–neuron metabolic relationships: for better and for worse. Trends Neurosci 34, 76–87. https://doi.org/10.1016/j.tins.2010.12.001.

Allen, N.J., Eroglu, C., 2017. Cell biology of astrocyte-synapse interactions. Neuron 96, 697–708. https://doi.org/10.1016/j.neuron.2017.09.056.

Araque, A., Parpura, V., Sanzgiri, R.P., Haydon, P.G., Araque, A., Parpura, V., Sanzgiri, R. P., Haydon, P.G., 1999. Tripartite synapses: glia, the unacknowledged partner. Trends Neurosci 22, 208–215. https://doi.org/10.1016/S0166-2236(98)01349-6.

Banasr, M., Chowdhury, G.M.I., Terwilliger, R., Newton, S.S., Duman, R.S., Behar, K.L., Sanacora, G., 2010. Glial pathology in an animal model of depression: reversal of stress-induced cellular, metabolic and behavioral deficits by the glutamate-modulating drug riluzole. Mol. Psychiatr. 15, 501–511. https://doi.org/10.1038/mp.2008.106.

Bansal, Y., Fee, C., Misquitta, K.A., Codeluppi, S., Sibille, E., Berman, R.M., Coric, V., Sanacora, G., Banasr, M., 2021. Prophylactic efficacy of riluzole against anxiety- and depressive-like behaviors in two rodent stress models. bioRxiv. https://doi.org/10.1101/2020.08.07.242057, 2020.08.07.242057.

Blume, S.R., Padival, M., Urban, J.H., Rosenkranz, J.A., 2019. Disruptive effects of repeated stress on basolateral amygdala neurons and fear behavior across the estrous cycle in rats. Sci. Rep. 9, 12292. https://doi.org/10.1038/s41598-019-48683-3.

Boisvert, M.M., Erikson, G.A., Shokhirev, M.N., Allen, N.J., 2018. The aging astrocyte transcriptome from multiple regions of the mouse brain. Cell Rep 22, 269–285. https://doi.org/10.1016/j.celrep.2017.12.039.

Brennan, B.P., Hudson, J.I., Jensen, J.E., McCarthy, J., Roberts, J.L., Prescot, A.P., Cohen, B.M., Pope, H.G., Renshaw, P.F., Öngür, D., 2010. Rapid enhancement of glutamatergic neurotransmission in bipolar depression following treatment with riluzole. Neuropsychopharmacol. Off. Publ. Am. Coll. Neuropsychopharmacol. 35, 834–846. https://doi.org/10.1038/npp.2009.191.

Bushong, E.A., Martone, M.E., Jones, Y.Z., Ellisman, M.H., 2002. Protoplasmic astrocytes in CA1 stratum radiatum occupy separate anatomical domains. J. Neurosci. 22, 183–192. https://doi.org/10.1523/JNEUROSCI.22-01-00183.2002.

Chattarji, S., Tomar, A., Suvrathan, A., Ghosh, S., Rahman, M.M., 2015. Neighborhood matters: divergent patterns of stress-induced plasticity across the brain. Nat. Neurosci. 18, 1364–1375. https://doi.org/10.1038/nn.4115.

Debono, M.W., Le Guern, J., Canton, T., Doble, A., Pradier, L., 1993. Inhibition by riluzole of electrophysiological responses mediated by rat kainate and NMDA receptors expressed in Xenopus oocytes. Eur. J. Pharmacol. 235, 283–289. https://doi.org/10.1016/0014-2999(93)90147-a.

Foy, M.R., Stanton, M.E., Levine, S., Thompson, R.F., 1987. Behavioral stress impairs long-term potentiation in rodent hippocampus. Behav. Neural. Biol. 48, 138–149. https://doi.org/10.1016/S0163-1047(87)90664-9.

dos S Frizzo, M.E., Dall'Onder, L.P., Dalcin, K.B., Souza, D.O., 2004. Riluzole enhances glutamate uptake in rat astrocyte cultures. Cell. Mol. Neurobiol. 24, 123–128. https://doi.org/10.1023/b:cemn.0000012717.37839.07.

Fullana, M.N., Ruiz-Bronchal, E., Ferrés-Coy, A., Juárez-Escoto, E., Artigas, F., Bortolozzi, A., 2019. Regionally selective knockdown of astroglial glutamate transporters in infralimbic cortex induces a depressive phenotype in mice. Glia 67, 1122–1137. https://doi.org/10.1002/glia.23593.

Fumagalli, E., Funicello, M., Rauen, T., Gobbi, M., Mennini, T., 2008. Riluzole enhances the activity of glutamate transporters GLAST, GLT1 and EAAC1. Eur. J. Pharmacol. 578, 171–176. https://doi.org/10.1016/j.ejphar.2007.10.023.

Geuze, E., Vermetten, E., Ruf, M., de Kloet, C.S., Westenberg, H.G.M., 2008. Neural correlates of associative learning and memory in veterans with posttraumatic stress disorder. J. Psychiatr. Res. 42, 659–669. https://doi.org/10.1016/j.jpsychires.2007.06.007.

Ghosh, S., Laxmi, T.R., Chattarji, S., 2013. Functional connectivity from the amygdala to the hippocampus grows stronger after stress. J. Neurosci. Off. J. Soc. Neurosci. 33, 7234–7244. https://doi.org/10.1523/JNEUROSCI.0638-13.2013.

Giacometti, L., Barker, J., 2020. Sex differences in the glutamate system: implications for addiction. Neurosci. Biobehav. Rev. 113, 157–168. https://doi.org/10.1016/j.neubiorev.2020.03.010.

Gilles, E.E., Schultz, L., Baram, T.Z., 1996. Abnormal corticosterone regulation in an immature rat model of continuous chronic stress. Pediatr. Neurol. 15, 114–119. https://doi.org/10.1016/0887-8994(96)00153-1.

Gould, E., Woolley, C.S., Frankfurt, M., McEwen, B.S., 1990. Gonadal steroids regulate dendritic spine density in hippocampal pyramidal cells in adulthood. J. Neurosci. 10, 1286–1291. https://doi.org/10.1523/JNEUROSCI.10-04-01286.1990.

Gourley, S.L., Espitia, J.W., Sanacora, G., Taylor, J.R., 2012. Antidepressant-like properties of oral riluzole and utility of incentive disengagement models of depression in mice. Psychopharmacology 219, 805–814. https://doi.org/10.1007/s00213-011-2403-4.

Govindarajan, A., Rao, B.S.S., Nair, D., Trinh, M., Mawjee, N., Tonegawa, S., Chattarji, S., 2006. Transgenic brain-derived neurotrophic factor expression causes both anxiogenic and antidepressant effects. Proc. Natl. Acad. Sci. Unit. States Am. 103, 13208–13213. https://doi.org/10.1073/pnas.0605180103.

Grosche, A., Grosche, J., Tackenberg, M., Scheller, D., Gerstner, G., Gumprecht, A., Pannicke, T., Hirrlinger, P.G., Wilhelmsson, U., Hüttmann, K., Härtig, W., Steinhäuser, C., Pekny, M., Reichenbach, A., 2013. Versatile and simple approach to determine astrocyte territories in mouse neocortex and Hippocampus. PLoS One 8, e69143. https://doi.org/10.1371/journal.pone.0069143.

Gupta, K., Chattarji, S., 2021. Sex differences in the delayed impact of acute stress on the amygdala. Neurobiol. Stress 14, 100292. https://doi.org/10.1016/j.ynstr.2020.100292.

Henneberger, C., Bard, L., Panatier, A., Reynolds, J.P., Kopach, O., Medvedev, N.I., Minge, D., Herde, M.K., Anders, S., Kraev, I., Heller, J.P., Rama, S., Zheng, K., Jensen, T.P., Sanchez-Romero, I., Jackson, C.J., Janovjak, H., Ottersen, O.P., Nagelhus, E.A., Oliet, S.H.R., Stewart, M.G., Nägerl, U.V., Rusakov, D.A., 2020. LTP induction boosts glutamate spillover by driving withdrawal of perisynaptic astroglia. Neuron 108, 919–936. https://doi.org/10.1016/j.neuron.2020.08.030 e11.

Herde, M.K., Bohmbach, K., Domingos, C., Vana, N., Komorowska-Müller, J.A., Passlick, S., Schwarz, I., Jackson, C.J., Dietrich, D., Schwarz, M.K., Henneberger, C., 2020. Local efficacy of glutamate uptake decreases with synapse size. Cell Rep 32, 108182. https://doi.org/10.1016/j.celrep.2020.108182.

Hubbard, J.A., Szu, J.I., Yonan, J.M., Binder, D.K., 2016. Regulation of astrocyte glutamate transporter-1 (GLT1) and aquaporin-4 (AQP4) expression in a model of epilepsy. Exp. Neurol. 283, 85–96. https://doi.org/10.1016/j.expneurol.2016.05.003.

Katoh-Semba, R., Asano, T., Ueda, H., Morishita, R., Takeuchi, I.K., Inaguma, Y., Kato, K., 2002. Riluzole enhances expression of brain-derived neurotrophic factor with consequent proliferation of granule precursor cells in the rat hippocampus. FASEB J. Off. Publ. Fed. Am. Soc. Exp. Biol. 16, 1328–1330. https://doi.org/10.1096/fj.02-0143fje.

Khakh, B.S., Sofroniew, M.V., 2015. Diversity of astrocyte functions and phenotypes in neural circuits. Nat. Neurosci. 18, 942–952. https://doi.org/10.1038/nn.4043.

Kitayama, N., Vaccarino, V., Kutner, M., Weiss, P., Bremner, J.D., 2005. Magnetic resonance imaging (MRI) measurement of hippocampal volume in posttraumatic stress disorder: a meta-analysis. J. Affect. Disord. 88, 79–86. https://doi.org/10.1016/j.jad.2005.05.014.

Lacomblez, L., Bensimon, G., Leigh, P.N., Guillet, P., Meininger, V., 1996. Dose-ranging study of riluzole in amyotrophic lateral sclerosis. Amyotrophic Lateral Sclerosis/Riluzole Study Group II. Lancet Lond. Engl. 347, 1425–1431. https://doi.org/10.1016/s0140-6736(96)91680-3.

Lowy, M.T., Gault, L., Yamamoto, B.K., 1993. Rapid communication: adrenalectomy attenuates stress-induced elevations in extracellular glutamate concentrations in the Hippocampus. J. Neurochem. 61, 1957–1960. https://doi.org/10.1111/j.1471-4159.1993.tb09839.x.

Luine, V., Gomez, J., Beck, K., Bowman, R., 2017. Sex differences in chronic stress effects on cognition in rodents. Pharmacol. Biochem. Behav., Sex differences on drugs affecting behavior 152, 13–19. https://doi.org/10.1016/j.pbb.2016.08.005.

MacVicar, B.A., Newman, E.A., 2015. Astrocyte regulation of blood flow in the brain. Cold Spring Harbor Perspect. Biol. 7, a020388. https://doi.org/10.1101/cshperspect.a020388.

Magariños, A.M., McEwen, B.S., 1995. Stress-induced atrophy of apical dendrites of hippocampal CA3c neurons: involvement of glucocorticoid secretion and excitatory amino acid receptors. Neuroscience 69, 89–98. https://doi.org/10.1016/0306-4522(95)00259-l.

McEwen, B.S., 1999. Stress and hippocampal plasticity. Annu. Rev. Neurosci. 22, 105–122. https://doi.org/10.1146/annurev.neuro.22.1.105.

McEwen, B.S., Bowles, N.P., Gray, J.D., Hill, M.N., Hunter, R.G., Karatsoreos, I.N., Nasca, C., 2015. Mechanisms of stress in the brain. Nat. Neurosci. 18, 1353–1363. https://doi.org/10.1038/nn.4086.

Mitra, R., Jadhav, S., McEwen, B.S., Vyas, A., Chattarji, S., 2005. Stress duration modulates the spatiotemporal patterns of spine formation in the basolateral amygdala. Proc. Natl. Acad. Sci. Unit. States Am. 102, 9371–9376. https://doi.org/10.1073/pnas.0504011102.

Murphy-Royal, C., Dupuis, J., Groc, L., Oliet, S.H.R., 2017. Astroglial glutamate transporters in the brain: regulating neurotransmitter homeostasis and synaptic transmission. J. Neurosci. Res. 95, 2140–2151. https://doi.org/10.1002/jnr.24029.

Murphy-Royal, C., Gordon, G.R., Bains, J.S., 2019. Stress-induced structural and functional modifications of astrocytes-Further implicating glia in the central response to stress. Glia 67, 1806–1820. https://doi.org/10.1002/glia.23610.

Naskar, S., Chattarji, S., 2019. Stress elicits contrasting effects on the structure and number of astrocytes in the amygdala versus Hippocampus. eneuro 6. https://doi.org/10.1523/ENEURO.0338-18.2019. ENEURO.0338-18.2019.

Padival, M., Quinette, D., Rosenkranz, J.A., 2013. Effects of repeated stress on excitatory drive of basal amygdala neurons in vivo. Neuropsychopharmacology 38, 1748–1762. https://doi.org/10.1038/npp.2013.74.

Pavlides, C., Nivón, L.G., McEwen, B.S., 2002. Effects of chronic stress on hippocampal long-term potentiation. Hippocampus 12, 245–257. https://doi.org/10.1002/hipo.1116.

Pawlak, R., Rao, B.S.S., Melchor, J.P., Chattarji, S., McEwen, B., Strickland, S., 2005. Tissue plasminogen activator and plasminogen mediate stress-induced decline of neuronal and cognitive functions in the mouse hippocampus. Proc. Natl. Acad. Sci. U.S.A. 102, 18201. https://doi.org/10.1073/pnas.0509232102.

Pereira, A.C., Gray, J.D., Kogan, J.F., Davidson, R.L., Rubin, T.G., Okamoto, M., Morrison, J.H., McEwen, B.S., 2017. Age and Alzheimer's disease gene expression profiles reversed by the glutamate modulator riluzole. Mol. Psychiatr. 22, 296–305. https://doi.org/10.1038/mp.2016.33.

Pillai, A.G., Anilkumar, S., Chattarji, S., 2012. The same antidepressant elicits contrasting patterns of synaptic changes in the amygdala vs Hippocampus. Neuropsychopharmacology 37, 2702–2711. https://doi.org/10.1038/npp.2012.135.

Pittenger, C., Coric, V., Banasr, M., Bloch, M., Krystal, J.H., Sanacora, G., 2008. Riluzole in the treatment of mood and anxiety disorders. CNS Drugs 22, 761–786. https://doi.org/10.2165/00023210-200822090-00004.

Proper, E.A., Hoogland, G., Kappen, S.M., Jansen, G.H., Rensen, M.G.A., Schrama, L.H., van Veelen, C.W.M., van Rijen, P.C., van Nieuwenhuizen, O., Gispen, W.H., de Graan, P.N.E., 2002. Distribution of glutamate transporters in the hippocampus of

patients with pharmaco-resistant temporal lobe epilepsy. Brain 125, 32–43. https://doi.org/10.1093/brain/awf001.

Rahman, M.M., Callaghan, C.K., Kerskens, C.M., Chattarji, S., O'Mara, S.M., 2016. Early hippocampal volume loss as a marker of eventual memory deficits caused by repeated stress. Sci. Rep. 6, 29127. https://doi.org/10.1038/srep29127.

Rauch, S.L., Whalen, P.J., Shin, L.M., McInerney, S.C., Macklin, M.L., Lasko, N.B., Orr, S. P., Pitman, R.K., 2000. Exaggerated amygdala response to masked facial stimuli in posttraumatic stress disorder: a functional MRI study. Biol. Psychiatr. 47, 769–776. https://doi.org/10.1016/S0006-3223(00)00828-3.

Reagan, L.P., Rosell, D.R., Wood, G.E., Spedding, M., Muñoz, C., Rothstein, J., McEwen, B.S., 2004. Chronic restraint stress up-regulates GLT-1 mRNA and protein expression in the rat hippocampus: reversal by tianeptine. Proc. Natl. Acad. Sci. Unit. States Am. 101, 2179. https://doi.org/10.1073/pnas.0307294101.

Reznikov, L.R., Grillo, C.A., Piroli, G.G., Pasumarthi, R.K., Reagan, L.P., Fadel, J., 2007. Acute stress-mediated increases in extracellular glutamate levels in the rat amygdala: differential effects of antidepressant treatment. Eur. J. Neurosci. 25, 3109–3114. https://doi.org/10.1111/j.1460-9568.2007.05560.x.

Roozendaal, B., McEwen, B.S., Chattarji, S., 2009. Stress, memory and the amygdala. Nat. Rev. Neurosci. 10, 423–433. https://doi.org/10.1038/nrn2651.

Rothstein, J.D., Dykes-Hoberg, M., Pardo, C.A., Bristol, L.A., Jin, L., Kuncl, R.W., Kanai, Y., Hediger, M.A., Wang, Y., Schielke, J.P., Welty, D.F., 1996. Knockout of glutamate transporters reveals a major role for astroglial transport in excitotoxicity and clearance of glutamate. Neuron 16, 675–686. https://doi.org/10.1016/S0896-6273(00)80086-0.

Rothstein, J.D., Van Kammen, M., Levey, A.I., Martin, L.J., Kuncl, R.W., 1995. Selective loss of glial glutamate transporter GLT-1 in amyotrophic lateral sclerosis. Ann. Neurol. 38, 73–84. https://doi.org/10.1002/ana.410380114.

Sanacora, G., Kendell, S.F., Levin, Y., Simen, A.A., Fenton, L.R., Coric, V., Krystal, J.H., 2007. Preliminary evidence of riluzole efficacy in antidepressant-treated patients with residual depressive symptoms. Biol. Psychiatr. 61, 822–825. https://doi.org/10.1016/j.biopsych.2006.08.037.

Sapolsky, R.M., Krey, L.C., McEwen, B.S., 1983. The adrenocorticol stress-response in the aged male rat: impairment of recovery from stress. Exp. Gerontol. 18, 55–64. https://doi.org/10.1016/0531-5565(83)90051-7.

Savtchenko, L.P., Zheng, K., Rusakov, D.A., 2021. Buffering by transporters can spare geometric hindrance in controlling glutamate escape. Front. Cell. Neurosci. 15.

Schindelin, J., Arganda-Carreras, I., Frise, E., Kaynig, V., Longair, M., Pietzsch, T., Preibisch, S., Rueden, C., Saalfeld, S., Schmid, B., Tinevez, J.-Y., White, D.J., Hartenstein, V., Eliceiri, K., Tomancak, P., Cardona, A., 2012. Fiji: an open-source platform for biological-image analysis. Nat. Methods 9, 676–682. https://doi.org/10.1038/nmeth.2019.

Seney, M.L., Glausier, J., Sibille, E., 2022. Large-scale transcriptomics studies provide insight into sex differences in depression. Biol. Psychiatr. 91, 14–24. https://doi.org/10.1016/j.biopsych.2020.12.025.

Sheline, Y.I., Barch, D.M., Donnelly, J.M., Ollinger, J.M., Snyder, A.Z., Mintun, M.A., 2001. Increased amygdala response to masked emotional faces in depressed subjects

resolves with antidepressant treatment: an fMRI study. Biol. Psychiatr. 50, 651–658. https://doi.org/10.1016/S0006-3223(01)01263-X.

Shors, T.J., Chua, C., Falduto, J., 2001. Sex differences and opposite effects of stress on dendritic spine density in the male versus female Hippocampus. J. Neurosci. 21, 6292–6297. https://doi.org/10.1523/JNEUROSCI.21-16-06292.2001.

Shukla, A., Chattarji, S., 2021. Stressed rats fail to exhibit avoidance reactions to innately aversive social calls. Neuropsychopharmacology 1–11. https://doi.org/10.1038/s41386-021-01230-z.

Sofroniew, M.V., Vinters, H.V., 2010. Astrocytes: biology and pathology. Acta Neuropathol. 119, 7–35. https://doi.org/10.1007/s00401-009-0619-8.

Spangler, P.T., West, J.C., Dempsey, C.L., Possemato, K., Bartolanzo, D., Aliaga, P., Zarate, C., Vythilingam, M., Benedek, D.M., 2020. Randomized controlled trial of riluzole augmentation for posttraumatic stress disorder: efficacy of a glutamatergic modulator for antidepressant-resistant symptoms. J. Clin. Psychiatr. 81, 20m13233. https://doi.org/10.4088/JCP.20m13233.

Suvrathan, A., Bennur, S., Ghosh, S., Tomar, A., Anilkumar, S., Chattarji, S., 2014. Stress enhances fear by forming new synapses with greater capacity for long-term potentiation in the amygdala. Philos. Trans. R. Soc. B Biol. Sci. 369, 20130151. https://doi.org/10.1098/rstb.2013.0151.

Tanaka, K., Watase, K., Manabe, T., Yamada, K., Watanabe, M., Takahashi, K., Iwama, H., Nishikawa, T., Ichihara, N., Kikuchi, T., Okuyama, S., Kawashima, N., Hori, S., Takimoto, M., Wada, K., 1997. Epilepsy and exacerbation of brain injury in mice lacking the glutamate transporter GLT-1. Science. https://doi.org/10.1126/science.276.5319.1699.

Vyas, A., Mitra, R., Shankaranarayana Rao, B.S., Chattarji, S., 2002. Chronic stress induces contrasting patterns of dendritic remodeling in hippocampal and amygdaloid neurons. J. Neurosci. 22, 6810. https://doi.org/10.1523/JNEUROSCI.22-15-06810.2002.

Wellman, C.L., Bangasser, D.A., Bollinger, J.L., Coutellier, L., Logrip, M.L., Moench, K. M., Urban, K.R., 2018. Sex differences in risk and resilience: stress effects on the neural substrates of emotion and motivation. J. Neurosci. 38, 9423–9432. https://doi.org/10.1523/JNEUROSCI.1673-18.2018.

Woon, F.L., Hedges, D.W., 2009. Amygdala volume in adults with posttraumatic stress disorder: a meta-analysis. J. Neuropsychiatry Clin. Neurosci. 21, 5–12. https://doi.org/10.1176/jnp.2009.21.1.5.

Yasmin, F., Saxena, K., McEwen, B.S., Chattarji, S., 2016. The delayed strengthening of synaptic connectivity in the amygdala depends on NMDA receptor activation during acute stress. Phys. Rep. 4, e13002 https://doi.org/10.14814/phy2.13002.

Zhou, B., Zuo, Y., Jiang, R., 2019. Astrocyte morphology: diversity, plasticity, and role in neurological diseases. CNS Neurosci. Ther. 25, 665–673. https://doi.org/10.1111/cns.13123.

Zona, C., Cavalcanti, S., De Sarro, G., Siniscalchi, A., Marchetti, C., Gaetti, C., Costa, N., Mercuri, N., Bernardi, G., 2002. Kainate-induced currents in rat cortical neurons in culture are modulated by riluzole. Synap. N. Y. N 43, 244–251. https://doi.org/10.1002/syn.10040.